Electronic structure of rhombohedral Ti_2O_3

1996 J. Phys.: Condens. Matter 8 5987

(http://iopscience.iop.org/0953-8984/8/33/007)

J. Phys.: Condens. Matter **8** (1996) 5987–5995. Printed in the UK

Electronic structure of rhombohedral Ti_2O_3

L F Mattheiss
AT&T Bell Laboratories, Murray Hill, NJ 07974, USA

Received 14 February 1996

Abstract. The band properties of corundum-phase Ti_2O_3 have been calculated in the local-density approximation with the use of the linear augmented-plane-wave method. The results consist of low-lying O 2p states and a partially filled t_{2g} complex near E_F where metallic behaviour originates from overlapping a_{1g} and e_g^π subbands. Decreasing the c/a ratio (even beyond the observed low-temperature value) reduces but does *not* eliminate this a_{1g}–e_g^π band overlap, thereby precluding a band explanation for the metal–insulator transition that is observed in this system with no accompanying structural distortion.

The metal–insulator (M–I) transition in corundum-type Ti_2O_3, which was discovered by Morin [1] in 1959, differs from that observed in most other transition-metal oxide systems in that the transition is 'gradual' rather than 'sharp', extending over a relatively broad (about 250 K) temperature range. There have been long-standing disputes [2] regarding the origin and nature of this transition. While these issues have not yet been entirely resolved, the results of early neutron spin-flip scattering experiments [3] have ruled out any mechanisms that are based on magnetic-ordering phenomena. At present, the generally accepted view is that the M–I transition in rhombohedral Ti_2O_3 is caused by an anomalous decrease in the c/a ratio with temperature which shifts key energy-band states near E_F in such a way that a small (about 0.1 eV) semiconductor gap [2] is opened between the previously overlapping a_{1g} and e_g^π subbands of the Ti 3d manifold [4].

Ti_2O_3 shares many physical properties and characteristics with its isostructural vanadium counterpart, V_2O_3. Vanadium sesquioxide, which was extensively studied in the late 1960s and early 1970s, is generally regarded [5] as the canonical Mott–Hubbard system where the Coulomb interactions between conduction electrons produce a M–I transition that is inexplicable in terms of conventional one-electron band theory. In particular, both compounds share the corundum-type structure and exhibit a M–I transition [2] with no evidence for an accompanying structural distortion or onset of magnetic ordering. However, an anomaly in the c/a ratio is observed in both materials as the temperature is varied through the range of the M–I transition. The M–I transitions in both Ti_2O_3 and V_2O_3 are found to exhibit 'sluggish' characteristics. In the case of Ti_2O_3, the M–I transition not only extends over a broad (about 250 K) temperature interval, but also exhibits a time dependence [1]. Similarly, it has been noted that high-temperature NMR data [6] for V_2O_3 exhibit lineshape changes that extend over 12 h periods. This has led to the observation 'that the kinetics of the M–I phase transition in pure V_2O_3 is slow' [6].

In a previous theoretical study [7] of the V_2O_3 electronic structure, it was proposed that the structural and resistivity anomalies that are generally attributed to a Mott transition in V_2O_3 may arise instead from 'interstitial' defects where V or other dopants occupy NiAs-type cation sites that should be vacant in the corundum structure. According to this picture, the observed 'sluggish' behaviour could reflect the thermally induced tunnelling of

0953-8984/96/335987+09$19.50

Ti or V ions through the shared octahedral faces that separate neighbouring corundum and vacancy sites. The purpose of the present investigation is to help to resolve some of the many lingering questions that remain regarding the electronic properties of Ti_2O_3. With this objective, state-of-the-art first-principles band calculations have been carried out for corundum-phase Ti_2O_3. At present, the only available band-structure results for this system have been derived either from empirical [4, 9] or simplified tight-binding treatments [8].

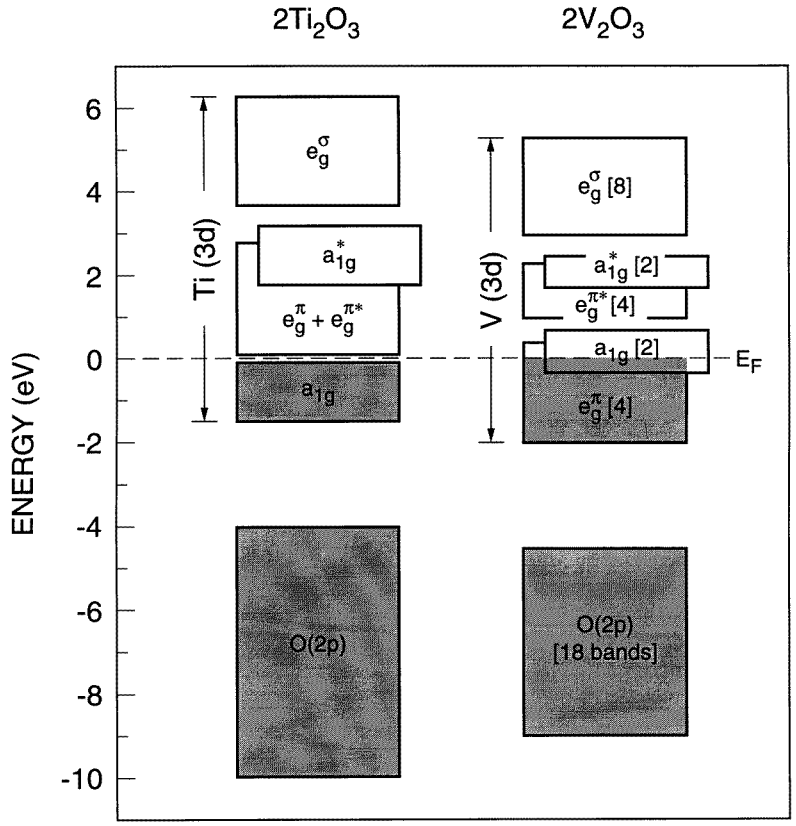

Figure 1. Comparison of the empirically derived band models for Ti_2O_3 and V_2O_3 [4, 9].

A schematic representation of the empirically derived band properties for V_2O_3 and Ti_2O_3 is presented in figure 1. The results for Ti_2O_3 feature a low-lying O 2p complex which is separated by an approximately 2 eV gap from the partially filled Ti 3d bands. The nearly octahedral coordination of the O atoms around the Ti atoms (figure 2) splits the Ti 3d levels into a lower t_{2g} manifold and an upper e_g complex. According to this model, a slight trigonal distortion of the TiO_6 octahedra (which is consistent with the rhombohedral symmetry of the corundum structure) further splits the t_{2g} subbands into non-degenerate a_{1g} and doubly degenerate e_g levels. The a_{1g} orbitals, which have $d_{3z^2-r^2}$ character, form (ddσ)-type bonds between the pairs of Ti atoms within the face-sharing octahedra that occur along the c axis in figure 2. The resulting bonding (a_{1g}) and antibonding (a_{1g}^*) combinations of bands are split to an extent that they essentially bracket the intermediate π-bonding e_g^π–$e_g^{\pi*}$ complex. In particular, the Ti_2O_3 semiconductor gap is expected to occur between the filled a_{1g} and the empty $e_g^\pi - e_g^{\pi*}$ subbands (which are often combined

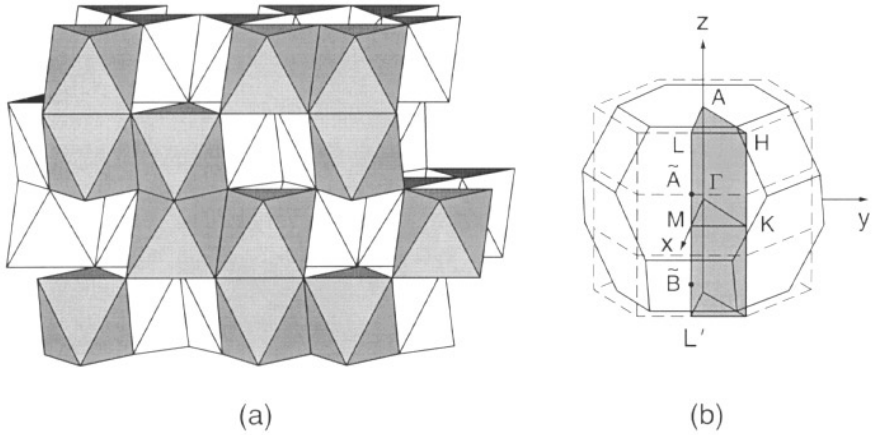

Figure 2. (a) Simplified view of the rhombohedral corundum structure as a linked network of NiAs-type face-sharing TiO_6 octahedra with ordered Ti vacancies; (b) rhombohedral BZ (——) and an equivalent hexagonally-shaped irreducible wedge.

below and denoted collectively by e_g^π). According to the Van Zandt–Honig–Goodenough [4] scenario, the increase in c/a with increasing temperature reduces the strength of the (ddσ)-type interactions between neighbouring $d_{3z^2-r^2}$ orbitals, thereby decreasing the a_{1g}–a_{1g}^* separation until the low-temperature semiconductor gap is finally eliminated.

In order to check the validity of this simple and appealing model for the M–I transition in Ti_2O_3, a scalar-relativistic version [10] of the linear augmented-plane-wave (LAPW) method [11] has been applied to calculate the band structure of corundum-phase Ti_2O_3 in the local-density approximation (LDA) [12]. As discussed below, the principal result of this study is that, while the a_{1g}–e_g^π band overlap in Ti_2O_3 is reduced by a decreasing c/a ratio, it is not entirely eliminated. It is concluded that the M–I transition in Ti_2O_3 cannot be explained in terms of a one-electron band picture. This suggests that it may be necessary to consider electron correlation effects or the presence of intrinsic defects such as titanium 'interstitials' in the search for a satisfactory explanation of this phenomenon.

A simplified view of the corundum structure is shown in figure 2(a). Here, pairs of face-sharing TiO_6 octahedra are linked via edge and vertex sharing to form a three-dimensional network with overall rhombohedral symmetry. In the resulting corundum structure, which has the $R\bar{3}c$ (D_{3d}^6) space-group symmetry, each primitive unit cell contains two Ti_2O_3 formula units. The observed Ti_2O_3 structural parameters [13] (i.e. $a = 5.158$ Å, $c = 13.611$ Å, $z(\mathrm{Ti}) = 0.3447$ and $x(\mathrm{O}) = 0.3106$) yield Ti–O bond lengths approximately in the 2.03–2.07 Å range while the Ti–Ti nearest-neighbour c-axis separation is about 2.58 Å. The lateral Ti–Ti bond lengths are about 16% larger (approximately 2.99 Å). The rhombohedral Brillouin zone (BZ) is shown in figure 2(b). The broken lines identify three hexagonal BZs for a hexagonal supercell which is three times larger, containing six Ti_2O_3 formula units. The standard labels Γ, M, K, A, L, and H are used to denote hexagonal BZ symmetry points. The points labelled Ã and B̃ identify points on the rhombohedral BZ surface that have been considered in previous tight-binding studies [8].

In the present calculations, exchange and correlation effects have been introduced with the use of the Wigner [14] interpolation formula. The LAPW basis has included plane waves with 14.4 Ryd cut-off (about 320 LAPWs per formula unit) and spherical-harmonic

terms up to $\ell = 6$ within the muffin-tin spheres. The crystalline charge density and potential have been expanded in terms of about 7000 plane waves in the interstitial region and lattice harmonics ($\ell_{max} = 4$) within the muffin-tin spheres. BZ averages have been calculated using a sample of 22 **k** points in the one-twelfth irreducible BZ wedge. The atomic Ti $3d^3\ 4s^1$ and O $2s^2\ 2p^4$ levels have been included as valence band states in these calculations while the remaining more tightly bound electrons have been treated via a rigid-core approximation [10].

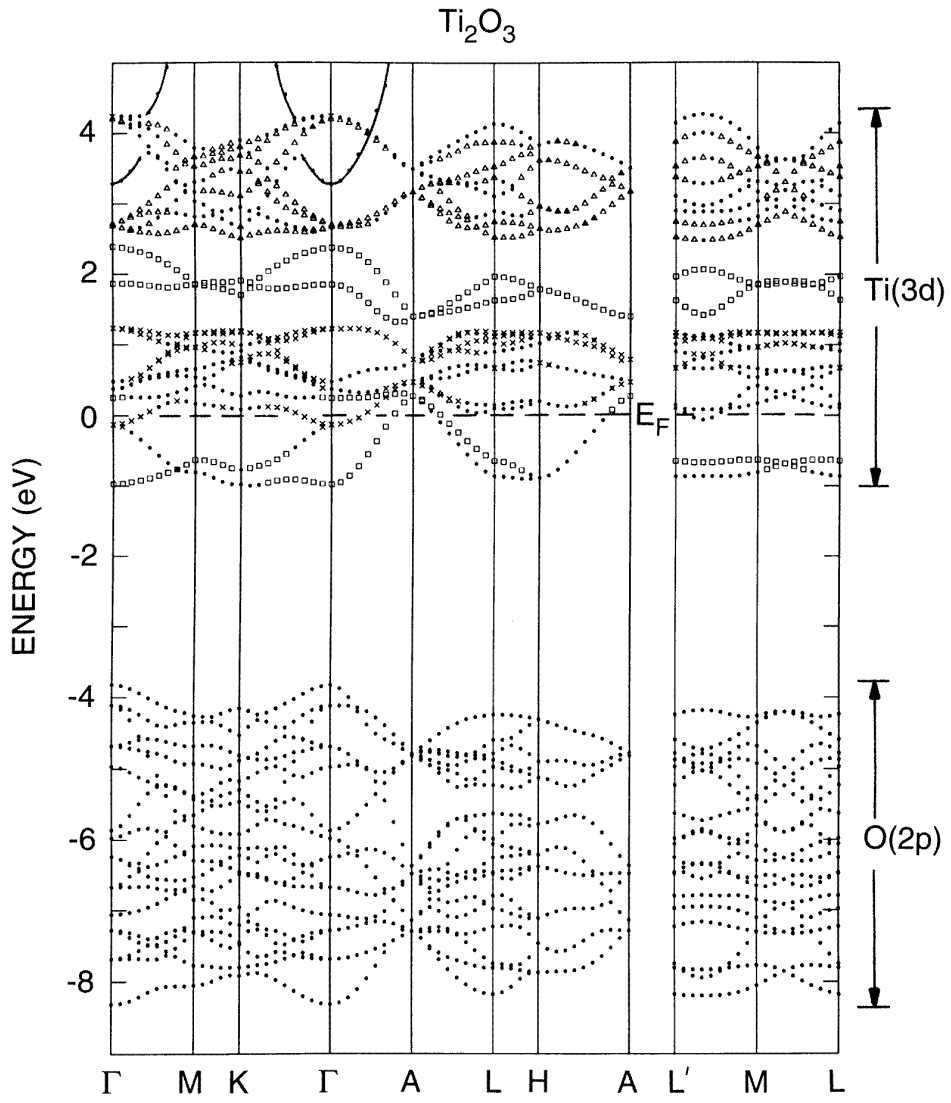

Figure 3. LAPW bands for rhombohedral Ti_2O_3 along symmetry lines of the hexagonally shaped BZ of figure 2.

The present LAPW band-structure results for Ti_2O_3 are plotted in figure 3 along lines on the surface of the hexagonal irreducible BZ wedge of figure 2(b). As the labelling to the

right indicates, the lowest 18 bands originate from the O 2p states while the Ti 3d levels form the upper complex of 20 bands. The bottom of the Ti 4s band, which has its minimum at Γ, is identified by the solid curves. In general, band counting is facilitated along the HA line where the bands are twofold degenerate. As the results show, the octahedral coordination at the Ti sites splits the 20 Ti 3d states into 12 partially filled t_{2g} bands and eight empty e_g-type states. Within the t_{2g} manifold, the uppermost pair of split-off subbands (which are centred near 2 eV) represent the a_{1g}^* states that have been depicted schematically in figure 1 as overlapping the e_g^π–$e_g^{\pi *}$ complex. However, since the calculated a_{1g} and e_g^π–$e_g^{\pi *}$ subbands do in fact overlap in the present LAPW results, metallic properties are predicted for rhombohedral Ti_2O_3.

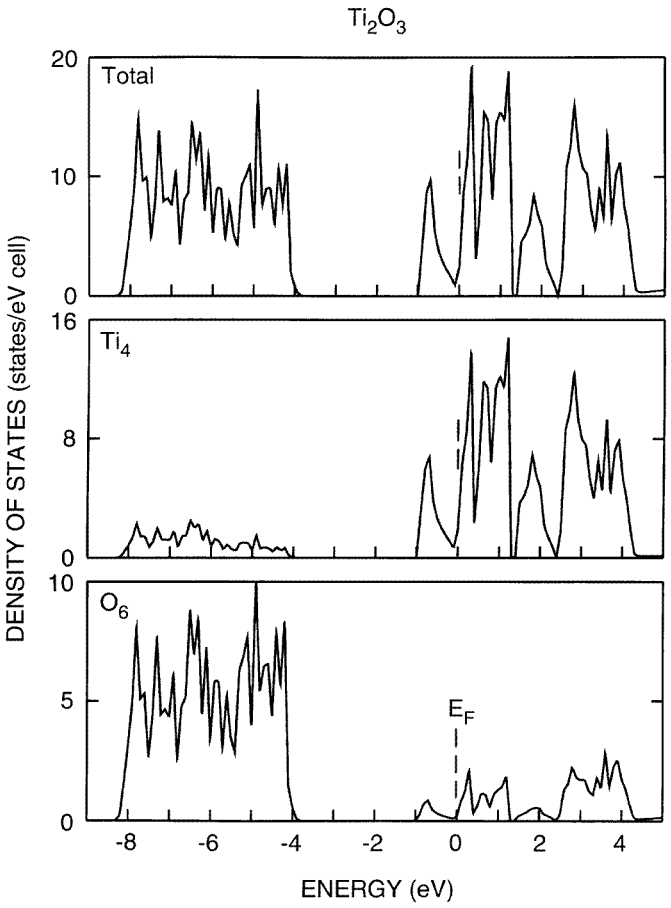

Figure 4. Total and muffin-tin projected DOS results for Ti_2O_3.

The density-of-states (DOS) results in figure 4 provide a more general overview of the Ti_2O_3 electronic properties. The Fermi level coincides with the low-energy shoulder of a DOS peak that originates from the e_g^π-subband edge. The a_{1g}–e_g^π band overlap (about 0.5 eV) is such that approximately 0.12 holes per cell occur in the nearly filled a_{1g} subband and these are compensated by about 0.12 electrons that occupy the corresponding e_g^π manifold. The calculated value for the Ti_2O_3 DOS at E_F is $N(E_F) \approx 2.4$ states eV^{-1}/cell. This is

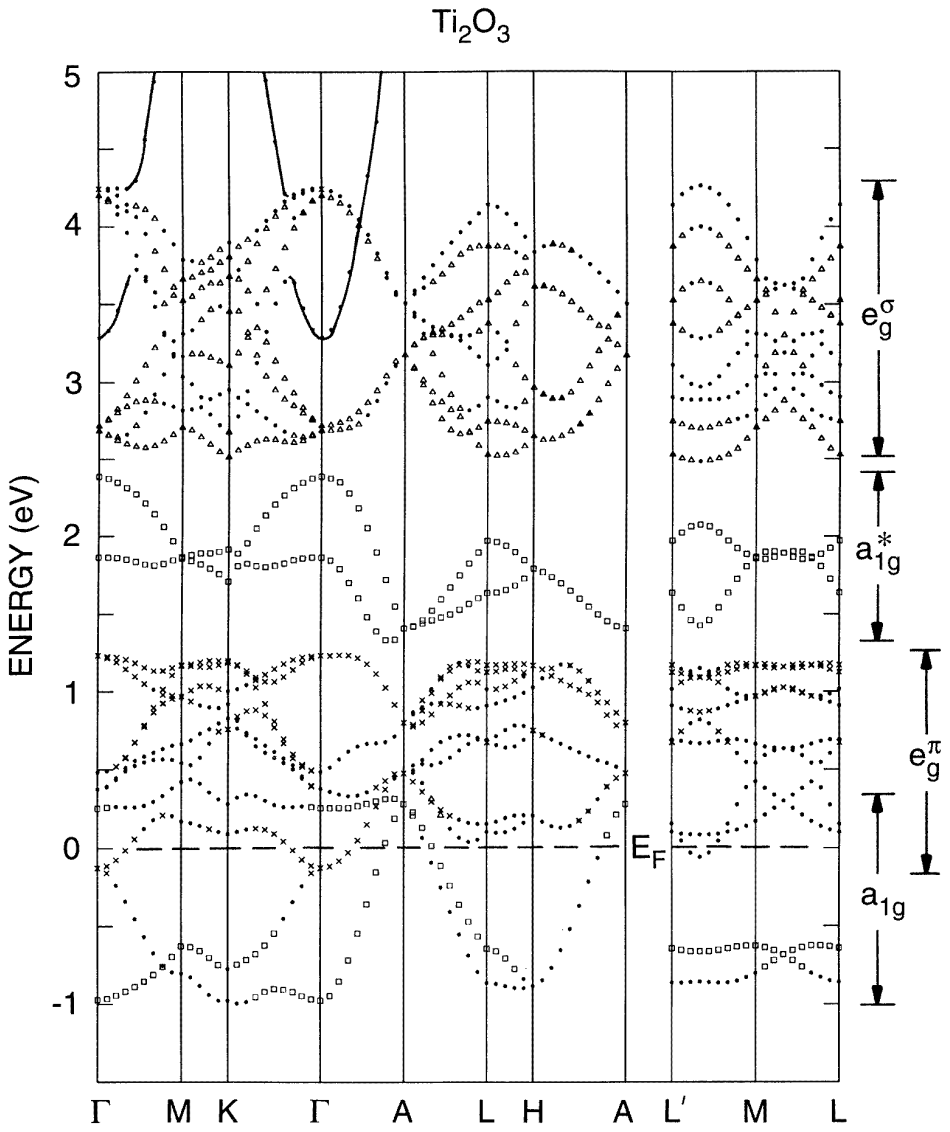

Figure 5. An expanded plot of the Ti 3d bands for Ti_2O_3, including the lower t_{2g} (i.e. the a_{1g}, e_g^π and a_{1g}^* subbands) and the upper e_g^σ manifolds. Open squares, crosses, and open triangles identify bands containing at least 40% $d_{3z^2-r^2}$, d_{xy,x^2-y^2} and $d_{xz,yz}$ orbital weight within the Ti muffin-tin spheres, respectively.

about a sixth of the value that has been calculated previously [7] for isostructural V_2O_3. As in the case of V_2O_3, the Ti 3d orbital weight is concentrated mainly in the t_{2g}–e_g energy range. This suggests that Ti 3d–O 2p hybridization effects are again diminished by a $\varepsilon_d - \varepsilon_p \approx$ 4 eV orbital-energy difference [7] and that the Ti 3d bandwidth originates mainly from (direct) d–d rather than (indirect) p–d interactions.

An expanded view of the Ti 3d bands is presented in figure 5. The labels to the right identify the energy ranges of the various subbands. Although the overall distribution of

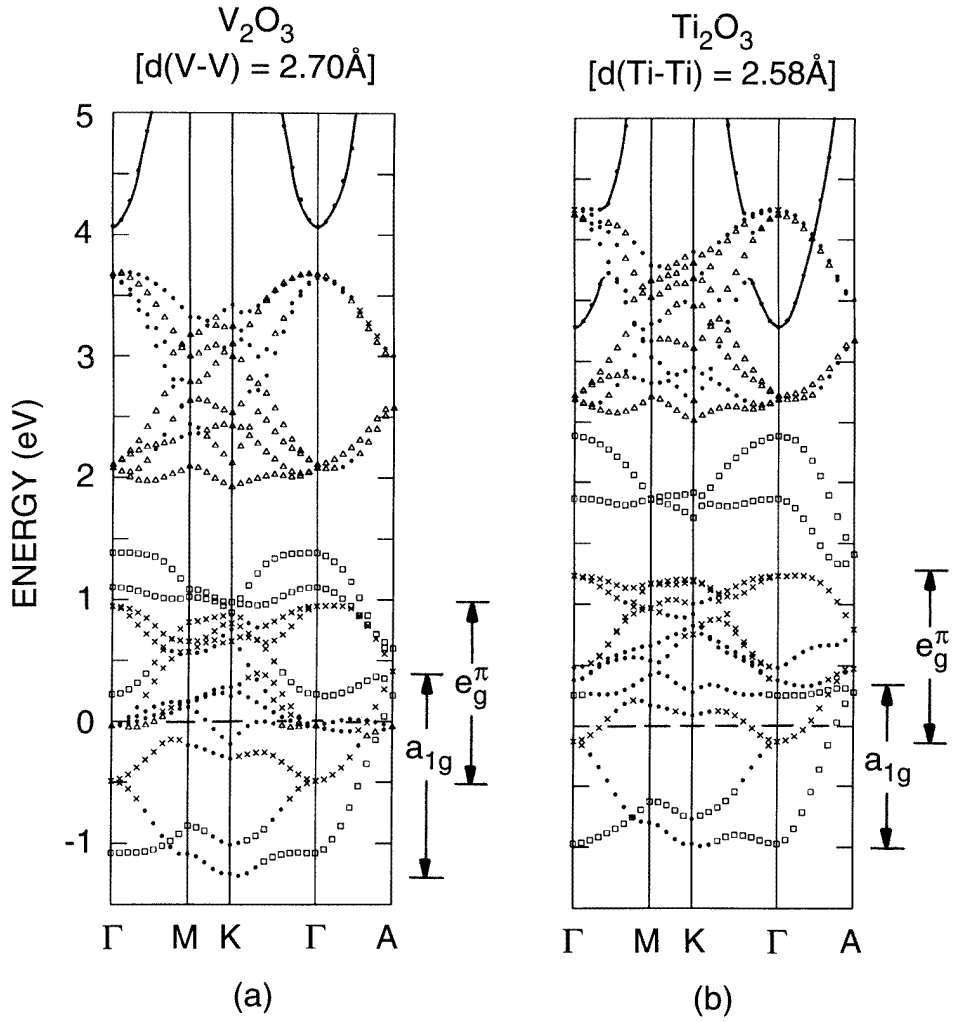

Figure 6. Comparison of the calculated a_{1g}–e_g^{π} band overlap in (a) V_2O_3 (observed structure), (b) Ti_2O_3 (observed structure) and (c) Ti_2O_3 with a modified structure containing a reduced Ti–Ti *c*-axis bond length (see text).

Ti 3d-band levels is in qualitative agreement with the semiempirical results in figure 1, it is evident that a band gap fails to materialize between the a_{1g}–e_g^{π} band complexes. Thus, the key feature of the Van Zandt–Honig–Goodenough [4] model for the M–I transition in Ti_2O_3 is not confirmed by the present LAPW results. Since the present Ti_2O_3 calculations are based on the room-temperature Ti_2O_3 structural parameters [13] (i.e. below the M–I transition), a semiconductor gap would be expected in this system, provided that it is not hidden by the 'band gap' problem [15] of LDA. In this regard, it is noted that the results of previous calculations for transition-metal compounds such as $CrSi_2$ [16] and FeSi [17] have yielded semiconductor gaps (about 0.30 eV and 0.11 eV, respectively) which are only approximately 15–20% smaller than observed values. This suggests that the tendency of LDA to underestimate band gaps is less severe in d-band materials such as Ti_2O_3 than in

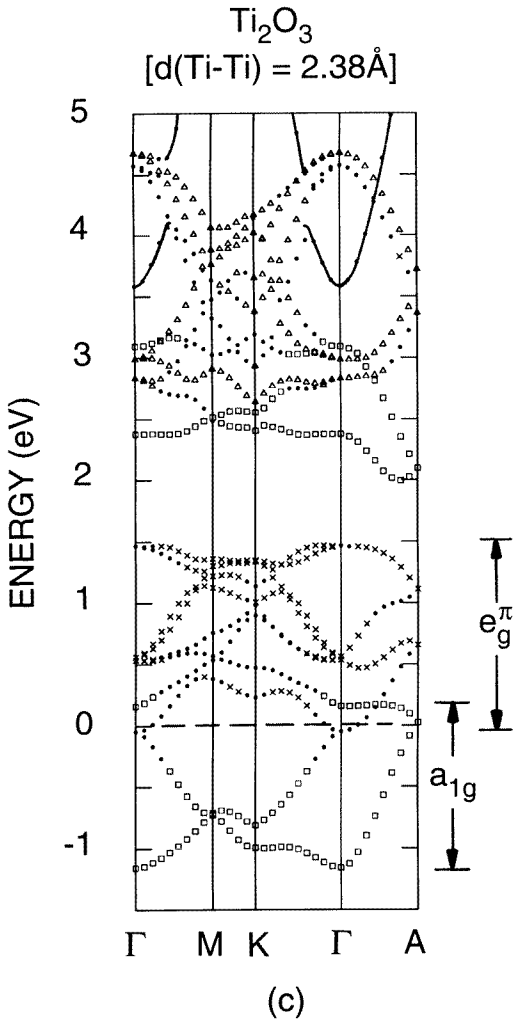

Figure 6. (Continued)

s–p bonded semiconductors. The rationale is that the similar d-type characteristics on both sides of the semiconductor gap may serve to minimize the non-local many-body corrections to LDA in such systems when compared with tetrahedrally bonded semiconductors [18]. Of course, it may turn out that Ti_2O_3 is an exception to this rule.

It is interesting to explore whether a further decrease in the c/a ratio (or, equivalently, in the nearest-neighbour Ti–Ti *c*-axis bond distance) will eventually open a semiconductor gap in Ti_2O_3. The results of an additional calculation for Ti_2O_3 in which each Ti has been displaced toward its *c*-axis neighbour by 0.1 Å are shown in figure 6(c). The corresponding results for V_2O_3 and Ti_2O_3 with their observed geometries are shown in figures 6(a) and 6(b), respectively. The approximate 7.8% decrease in the Ti–Ti *c*-axis bond distance (from about 2.58 Å to about 2.38 Å) is about three times larger than the approximate 2.6% change that occurs over the temperature range of the Ti_2O_3 M–I transition [19]. It is clear from the results in figure 6 that the calculated a_{1g}–e_g^π band overlap decreases systematically in V_2O_3

and Ti_2O_3 as the V–V and Ti–Ti bond distances are reduced. However, it appears that an unphysically small value of d(Ti–Ti) $\approx$ 2.2 Å would be required to open a semiconductor gap in Ti_2O_3.

In summary, the results of LAPW band calculations for corundum-phase Ti_2O_3 yield metallic properties that originate from overlapping a_{1g}–e_g^{π} bands. While this band overlap tends to decrease as the c/a ratio and the nearest-neighbour Ti–Ti bond distances are reduced, an unphysically small Ti–Ti separation of about 2.2 Å would be required in order to open a semiconductor gap in this system. This suggests that either electron–electron correlation effects or interstitial Ti defects, similar to those proposed previously [7] for V_2O_3, may provide the key to understanding the M–I transition in Ti_2O_3.

References

[1] Morin F J 1959 *Phys. Rev. Lett.* **3** 34
[2] For a review and comprehensive guide to the literature, see Honig J M and Van Zandt L L 1975 *Ann. Rev. Mater. Sci.* **5** 225
[3] Moon R M, Riste T, Koehler W C and Abrahams S C 1969 *J. Appl. Phys.* **40** 1445
[4] Van Zandt L L, Honig J M and Goodenough J B 1968 *J. Appl. Phys.* **39** 594
[5] McWhan D B, Rice T M and Remeika J P 1969 *Phys. Rev. Lett.* **23** 1384
[6] Kerlin A L, Nagasawa H and Jerome D 1973 *Solid State Commun.* **13** 1125
[7] Mattheiss L F 1994 *J. Phys.: Condens. Matter* **6** 6477
[8] Nebenzahl I and Weger M 1971 *Phil. Mag.* **24** 1119
Ashkenazi J and Chuchem T 1975 *Phil. Mag.* **32** 763
[9] Goodenough J B 1972 *Prog. Solid State Chem.* **5** 145
[10] Mattheiss L F and Hamann D R 1986 *Phys. Rev.* B **33** 823
[11] Andersen O K 1975 *Phys. Rev.* B **12** 3060
[12] Hohenberg P and Kohn W 1964 *Phys. Rev.* B **136** 864
Kohn W and Sham L J 1965 *Phys. Rev.* A **140** 1133
[13] Vincent M G, Yoon K, Grüttner A and Ashkenazi J 1980 *Acta. Crystallogr.* A **36** 803
[14] Wigner E 1934 *Phys. Rev.* **46** 1002
[15] Sham L J and Schlüter M 1983 *Phys. Rev. Lett.* **51** 1888; 1985 *Phys. Rev.* B **32** 3883
[16] Mattheiss L F 1991 *Phys. Rev.* B **43** 1863
[17] Mattheiss L F 1993 *Phys. Rev.* B **47** 13 114
[18] Godby R N, Schlüter M and Sham L J 1986 *Phys. Rev. Lett.* **56** 2415; 1987 *Phys. Rev.* B **36** 6497
[19] Robinson W R 1974 *J. Solid State Chem.* **9** 255